HHS Public Access

Author manuscript

Dev Biol. Author manuscript; available in PMC 2018 January 15.

Published in final edited form as:

Dev Biol. 2017 January 15; 421(2): 245–257. doi:10.1016/j.ydbio.2016.11.009.

Supt20 is Required for Development of the Axial Skeleton

Sunita Warrier[1], **Samer Nuwayhid**[1], **Julia A. Sabatino**[1], **Kelsey F. Sugrue**[1,2], and **Irene E. Zohn**[1,*]

[1]Center for Neuroscience Research, Children's Research Institute, Children's National Medical Center, Washington, DC 20010

[2]Institute for Biomedical Sciences, The George Washington University, Washington, DC 20052, USA

Abstract

Somitogenesis and subsequent axial skeletal development is regulated by the interaction of pathways that determine the periodicity of somite formation, rostrocaudal somite polarity and segment identity. Here we use a hypomorphic mutant mouse line to demonstrate that Supt20 (Suppressor of Ty20) is required for development of the axial skeleton. Supt20 hypomorphs display fusions of the ribs and vertebrae at lower thoracic levels along with anterior homeotic transformation of L1 to T14. These defects are preceded by reduction of the rostral somite and posterior shifts in Hox gene expression. While cycling of Notch target genes in the posterior presomitic mesoderm (PSM) appeared normal, expression of Lfng was reduced. In the anterior PSM, Mesp2 expression levels and cycling were unaffected; yet, expression of downstream targets such as Lfng, Ripply2, Mesp1 and Dll3 in the prospective rostral somite was reduced accompanied by expansion of caudal somite markers such as EphrinB2 and Hes7. Supt20 interacts with the Gcn5-containing SAGA histone acetylation complex. Gcn5 hypomorphic mutant embryos show similar defects in axial skeletal development preceded by posterior shift of Hoxc8 and Hoxc9 gene expression. We demonstrate that Gcn5 and Supt20 hypomorphs show similar defects in rostral-caudal somite patterning potentially suggesting shared mechanisms.

Keywords

Supt20; Gcn5; Somitogenesis; Somite patterning; Hox code

Introduction

The segmented architecture of the vertebrate axial skeleton originates during embryogenesis from the metameric organization of transient embryonic structures known as somites. Somitogenesis and subsequent axial skeletal development is regulated by the interaction of

* Correspondence to Irene E. Zohn, Center for Neuroscience Research, Children's Research Institute, Children's National Medical Center, Washington, DC, 20010, USA. Phone: 01-202-476-2106, Fax: 01-202-476-4988, izohn@cnmcresearch.org.

pathways that determine the periodicity of somite formation, rostrocaudal somite polarity and segment identity. Following gastrulation, somites form in a rostral-to-caudal progression as cells of the anterior presomitic mesoderm (PSM) undergo periodic mesenchyme to epithelial transformations. Interaction of molecular oscillators known as the “segmentation clock” in the posterior PSM regulates periodicity of somite formation with graded signals of a 'wavefront' (first proposed in (Cooke and Zeeman, 1976) and recently reviewed in (Dequeant and Pourquie, 2008; Hubaud and Pourquie, 2014). At the determination front in the anterior PSM, interaction of signals of the segmentation clock and wavefront culminates in acquisition of rostrocaudal polarity and segment identity prior physical formation of the somites (reviewed in (Hubaud and Pourquie, 2014; Iimura et al., 2009; Saga, 2012). As somites mature, they compartmentalize into the dermomyotome and sclerotome that gives rise to axial muscles and dermis of the back or elements of the axial skeleton, respectively (reviewed in (Christ et al., 2004; Yusuf and Brand-Saberi, 2006).

The segmentation clock in the posterior PSM controls the periodicity of somite formation. This clock can be visualized by the oscillatory expression of components of Notch, Wnt and FGF pathways that occur in cycles once for each somite formed (Aulehla and Johnson, 1999; Aulehla et al., 2003; Bessho et al., 2001; Bone et al., 2014; Dequeant et al., 2006; Forsberg et al., 1998; Ishikawa et al., 2004; McGrew et al., 1998; Niwa et al., 2007; Palmeirim et al., 1997). Cyclic activation of these pathways results from activation of negative feedback loops (reviewed in (Hubaud and Pourquie, 2014). For instance, production of NICD1 (Notch1 intracellular domain) and subsequent negative feedback due to induced expression of Notch inhibitors such as Lfng and Hes7 sweeps across the PSM (Bessho et al., 2003; Dale et al., 2003; Morimoto et al., 2005). Oscillations in Notch pathway activation integrate with oscillations in Wnt and Fgf signaling into a complex regulatory network (Aulehla et al., 2003; Bone et al., 2014; Dequeant et al., 2006; Niwa et al., 2007; Wahl et al., 2007).

At the determination front, oscillatory gene expression ceases and cells of the somite primordia acquire a rostrocaudal pattern prior to physical formation of the somite (reviewed in (Hubaud and Pourquie, 2014; Saga, 2012). Positioning of the determination front requires cyclic activation of Notch, Wnt and Fgf pathways in the posterior PSM with an opposing gradient of Retinoic acid signaling culminating in expression of the bHLH transcription factor Mesp2 (Aulehla et al., 2003; Aulehla et al., 2008; Dubrulle et al., 2001; Dubrulle and Pourquie, 2004; Dunty et al., 2008; Goldbeter et al., 2007; Morimoto et al., 2005; Niederreither et al., 1997; Sakai et al., 2001; Yasuhiko et al., 2006). Mesp2 controls both segmentation and rostrocaudal patterning of the somite by regulating expression of a network of genes that specify rostral or caudal somite fates (Morimoto et al., 2005; Saga, 2007, 2012; Takahashi et al., 2003; Takahashi et al., 2000). Initially, Mesp2 is expressed in both the rostral and caudal portion of the next somite (S-1) to be formed (Morimoto et al., 2005; Oginuma et al., 2010; Takahashi et al., 2010; Takahashi et al., 2000). In the caudal half of S-1, Mesp2 initiates expression of its inhibitor Ripply1/2, restricting Mesp2 expression to the rostral domain (Takahashi et al., 2010). In the rostral somite, Mesp2 represses Notch signaling by inducing expression of Lfng and Dll3 and destabilizing the transcriptional co-activator MamL1 (Morimoto et al., 2005; Sasaki et al., 2011; Takahashi et al., 2010; Takahashi et al., 2003; Takahashi et al., 2000). In the caudal Mesp2-negative

somite, Notch signaling is active and Dll1 and Hes7 are expressed (Takahashi et al., 2003; Takahashi et al., 2000).

The rostrocaudal polarity of the somite is of particular importance for development of the sclerotome into elements of the axial skeleton. Some axial skeletal elements are formed through a process called resegmentation where the caudal sclerotome from one somite combines with the rostral sclerotome of the adjacent somite (reviewed in (Christ et al., 2007; Fleming et al., 2015; Scaal, 2016). The vertebral body and spinous process form through resegmentation, whereas the proximal ribs, neural arches and pedicles develop primarily from the caudal somite and the intervertebral disk and distal rib from the rostral somite (Aoyama and Asamoto, 2000; Bagnall et al., 1988; Evans, 2003; Ewan and Everett, 1992; Goldstein and Kalcheim, 1992). Establishment of somite polarity is also essential for proper migration of the neural crest and the motor nerve axons through the rostral somite (Bronner-Fraser, 2000; Keynes and Stern, 1984; Kuan et al., 2004). Thus the proper establishment of rostral-caudal somite polarity is crucial for the future segmentation of both the axial skeleton and peripheral nerves.

In addition to rostral-caudal pattern information, axial identity becomes fixed in the anterior PSM where anterior boundaries of Hox transcription factors are refined (reviewed in (Deschamps and van Nes, 2005; Iimura et al., 2009). Hox gene expression is initiated during gastrulation but as cells move through the PSM, Notch, Wnt, Fgf and Retinoic acid signals influence their final expression pattern (Cordes et al., 2004; Dubrulle et al., 2001; Greco et al., 1996; Ikeya and Takada, 2001; Kessel and Gruss, 1991; Lohnes et al., 1994; Partanen et al., 1998; Zakany et al., 2001). Based on the expression of unique Hox genes, somites will differentiate into vertebrae with distinct morphologies (Kessel and Gruss, 1991; Krumlauf, 1994) and alterations in expression of specific Hox genes result in homeotic transformations of the axial skeletal confined to particular axial levels (reviewed in (Wellik, 2009). For instance, mutations of Hoxc8 or Hoxc9 in mice result in rib fusions and homeotic transformations of the lower thoracic region including transformation of Lumbar (L1) vertebrae to Thoracic (T14) (Le Mouellic et al., 1992; Suemori et al., 1995; van den Akker et al., 2001). Furthermore, shifts in the anterior limit of Hox gene expression results in homeotic transformations. For example, Gcn5 is a histone acetyltransferase (HAT) that functions as an integral component of the SAGA (Spt Ada Gcn5 Acetyl transferase) multi-subunit histone-modifying complex (reviewed in (Wang and Dent, 2014). Hypomorphic mutation of Gcn5 results in axial patterning defects consisting of rib fusions and homeotic transformations of lumbar L1 to thoracic T14 vertebrae (Lin et al., 2008a). These axial skeletal defects are preceded by posterior shifts in the anterior boundary of Hoxc8 and Hoxc9 expression (Lin et al., 2008a).

There is considerable overlap between the pathways involved in gastrulation, mesoderm specification and somitogenesis. Consequently much of our knowledge of the pathways that regulate formation and patterning of the axial skeleton in the mouse initially arose from studies of hypomorphic mutants where gene function is not completely ablated. For example, null mutations of some Fgfs or Wnts results in severe gastrulation defects, precluding study of the gene function in somite formation (Ciruna and Rossant, 2001; Deng et al., 1994; Sun et al., 1999; Takada et al., 1994). However, hypomorphic mutations of these

genes allows for completion of gastrulation and analysis of gene functions in somite formation (Aulehla et al., 2003; Greco et al., 1996; Partanen et al., 1998). Full knockout of Wnt3a results in loss of paraxial mesoderm (Takada et al., 1994), whereas hypomorphic mutation of Wnt3a in vestigial tail (vt) mutants provides enough gene function for mesoderm development to proceed allowing analysis of in somite formation and vertebral patterning (Aulehla et al., 2003; Greco et al., 1996). Similarly, Fgfr1 and Fgf8 mutant embryos show impaired migration of mesoderm through the primitive streak and subsequent mesoderm development (Ciruna and Rossant, 2001; Deng et al., 1994; Sun et al., 1999). Generation of a hypomorphic Fgfr1 allele reveals a key role for Fgfr1 in regulation of Hox gene expression and axial skeletal patterning (Partanen et al., 1998). Subsequent studies involving conditional deletion of Fgfr1 or Fgf8/Fgf4 after mesoderm migration confirmed the role of this pathway in somite formation and axial patterning (Naiche et al., 2011; Wahl et al., 2007). These studies demonstrate that somite defects in hypomorphs were not exclusively due to residual defects of gastrulation and mesoderm specification.

Analysis of other mouse lines further supports the utility of hypomorphic alleles in analysis of somite development. Fgf8 is required for Tbx6 expression in the PSM (Ciruna and Rossant, 2001) and analysis of hypomorphic Tbx6 mutants reveals Tbx6 is required for specification of posterior somites and rostral-caudal somite pattern (White et al., 2003). Mutation Actr2a;Actr2b result in defects in mesoderm formation (Oh and Li, 1997; Song et al., 1999), whereas reduce gene dosage of receptors in Actr2b or compound Actr2a and Actr2b mutants allows for mesoderm formation to occur and analysis of axial skeletal development (Oh et al., 2002). Finally, analysis of skeletal defects in hypomorphic mutations in Mesp2 or Notch pathway components allows for separation of the function of these genes in somite formation and rostrocaudal patterning (Cordes et al., 2004; Nomura-Kitabayashi et al., 2002; Schuster-Gossler et al., 2009). Together these studies illustrate the power of studying somite formation in hypomorphic mutant mouse lines to uncover later developmental functions of genes.

We previously described an ENU-induced hypomorphic mutation in Supt20 (suppressor of Ty20, also known as p38 mitogen activated protein kinase (MAPK) interacting protein (p38IP) or Fam48a) that results in an array of incompletely penetrant neural tube defects including spina bifida and exencephaly along with variable and very low penetrant gastrulation defects (Zohn et al., 2006). Among other functions, Supt20 is an essential core component of the Gcn5-containing SAGA complex (Grant et al., 1997; Nagy et al., 2009; Wang et al., 2008). While, full loss of Gcn5 function results in failure to form many mesoderm derivatives (Xu et al., 2000), Gcn5 hypomorphic mutants show axial skeleton defects in lower thoracic regions including rib fusions and homeotic transformations along with spina bifida and exencephaly (Bu et al., 2007; Lin et al., 2008a; Lin et al., 2008b). Here we demonstrate that like Gcn5, Supt20 hypomorphic mutants display rib and vertebrae fusions along with homeotic transformations of lower thoracic segments. Defects in axial skeletal development in Supt20 hypomorphic mutants are preceded by disruptions of the Mesp2-induced gene regulatory network at the determination front, alterations in rostrocaudal patterning of the somites and posterior shifts in Hoxc9 and Hoxc8 expression. Finally, we demonstrate that Gcn5 hypomorphic mutants show similar alterations in rostrocaudal patterning of the somites as Supt20 hypomorphs.

Materials and Methods

Mouse Strains and Analysis of Mutant Phenotypes. The Supt20^{drey}, Supt20$^{Gt(RRK304)Byg}$, Gcn5$^{flox(neo)}$ and Tg(BAT-lacZ)3Picc mouse lines were described previously (Lin et al., 2008a; Lin et al., 2008b; Maretto et al., 2003; Zohn et al., 2006). All strains were crossed onto a C3H background (C3H/HeNcrl) for at least 10 generations before analysis. Penetrance of gastrulation defects in Supt20^{hypo} mutant embryos was low and embryos with obvious gastrulation defects were excluded from analysis. Skeletal staining and whole-mount RNA in situs were performed as described (Hogan et al., 1994; Zohn et al., 2006). The following probes were used: Uncx4.1 (Mansouri et al., 1997), Tbx18 (Kraus et al., 2001), Dll1 (Bettenhausen et al., 1995), Hes7 (Bessho et al., 2001), Lfng (Evrard et al., 1998), Mesp2 (Saga et al., 1997), Mesp1 (Saga et al., 1996), Dll3 (Dunwoodie et al., 1997), Ripply2 (Biris et al., 2007), EphrinB2 (Bergemann et al., 1995), Brachyury (Rashbass et al., 1991), Wnt3a (Roelink and Nusse, 1991), Fgf8 (Tanaka et al., 1992), Spry4 (Zhang et al., 2001) and Hoxc8 and Hoxc9 (Burke et al., 1995). Immunohistochemical staining to detect alpha-neurofilament protein was performed as described (Davis et al., 1991) using the 2H3 antibody (Developmental Studies Hybridoma, University of Iowa) at a concentration of 1:250. Images were acquired using a Zeiss Lumar microscope with an Axiocam HRc camera (Zeiss) and Axiovision (4.6) software and processed using Adobe Photoshop (14.2). Figures were assembled in Adobe Illustrator (17.1.0). Western blot analysis was performed on E10.5 embryos lysed in RIPA buffer (Thermo Fisher Scientific #89901). Supt20 was detected using an anti-Supt20 antibody generated using a conserved recombinant peptide located within the first 300 amino acids of human Supt20 (Santa Cruz Biotechnology, sc-84118) with anti-Gapdh (Cell Signaling #2118) as a loading control. Westerns were visualized using the Odyssey Imaging System (LI-COR).

Results

Supt20 hypomorphic mutants display axial skeletal defects. Our previous studies showed that a genetrap allele of Supt20 (Supt20$^{Gt(RRK304)Byg}$) results in aberrant mesoderm organization in mouse embryos and embryonic lethality by E9.5 (Zohn et al., 2006). In contrast, a hypomorphic N-ethyl-N-nitrosourea (ENU)-induced mutation in Supt20 in the droopy eye (Supt20^{drey}) mutant mouse line results in variably penetrant exencephaly, spina bifida and very low penetrant gastrulation defects (Zohn et al., 2006). The drey mutation results in a T to C transition in the splice donor consensus sequence following exon 14 of the Supt20 gene (Zohn et al., 2006). Analysis of Supt20 transcripts produced in mutant embryos indicates that while some are normally spliced, the majority of transcripts utilize alternate splice donor sequences resulting in alternative splicing (Zohn et al., 2006). Sequencing of the aberrantly spliced transcripts reveals premature stop codons encountered at either 951 or 948 base pairs (Zohn et al., 2006). These alternatively spliced transcripts are predicted to results in truncation of the Supt20 protein from 531 to 316 or 317 amino acids and alteration of the predicted molecular weight from 60 kDa to 44 kDa. Western blot analysis using an anti-Supt20 antibody on embryo lysates from E10.5 wild type or Supt20$^{drey/+}$ and Supt20$^{drey/drey}$ embryos reveals a gene dosage-dependent reduction in the amount of wild type Supt20 protein produced (Supplemental Figure S1). The antibody used for this analysis is predicted to recognize truncated protein products and no alternative products were

detected in Supt20$^{drey/drey}$ embryos suggesting that alternatively spliced products are not stable. Further, no discernable phenotypes are observed in heterozygous Supt20$^{drey/+}$ animals suggesting if truncated products are present they do not have appreciable dominant-negative activities.

Since the frequency of developmental defects in Supt20$^{drey/drey}$ mutants was low (Zohn et al., 2006), to investigate the effects of reduced Supt20 activity on development of the axial skeleton we analyzed Supt20$^{drey/Gt(RRK304)Byg}$ transheterozygotes (hereafter referred to as Supt20 hypomorphs; Supt20^{hypo}) created by crossing Supt20$^{drey/+}$ with Supt20$^{Gt(RRK304)Byg/+}$. Examination of E15.5-16.5 Alcian Blue/Alizarin Red-stained Supt20^{hypo} skeletons revealed fusions of the ribs and vertebrae in the lower thoracic region (Figure 1). Cervical and the first 9 thoracic vertebrae and ribs (T1-T9) appeared normal in all skeletons examined (n=8). However, fusions were observed in the proximal ribs connected to thoracic vertebrae T10-T13 in approximately 75% of mutant embryos. (n=6/8). Fusions appeared without bias on both the left and right sides of the body axis (arrow heads in Figure 1B, C). Fusions of the pedicles and in some cases vertebral bodies were also observed (* in Figure 1E, F). In addition, 60% (5/8) of Supt20^{hypo} mutants showed transformation of the first lumbar (L1) to thoracic vertebrae (labeled as T14* in Figure 1B, C and E). Skeletal defects appeared in the mutants irrespective of whether they displayed neural tube defects.

Disrupted rostrocaudal polarity of somites in Supt20 hypomorphs. Fusions of axial skeletal elements can result from abnormal rostrocaudal patterning of the somites. The rostral and caudal division of somites provides a substrate for migration of the neural crest that transverse the rostral somite to form peripheral spinal nerves and axons (Bronner-Fraser, 2000; Keynes and Stern, 1984; Kuan et al., 2004). Thus, a normally segmented peripheral nerve pattern indicates the proper establishment of rostrocaudal somite polarity. To visualize segmentation of peripheral nerves, immunohistochemical staining was used to detect neurofilament protein. This analysis reveals normal periodicity of peripheral spinal nerves and dorsal root ganglia in E10.5 wild type embryos (Figure 2A; n=6). However, in Supt20 hypomorphs, the spinal nerves were thinner, misaligned and many nerve bundles failed to transverse the somite (Figure 2B; n=6).

To investigate whether skeletal fusions and abnormal segmentation of the peripheral nerves might stem from abnormal pattern of somites, the rostral and caudal sclerotome compartments were visualized by histology. In hematoxylin and eosin stained parasagittal sections of the lower thoracic region of E12.5 control embryos, the sclerotome presents as alternating dark and light stripes of rostral dense pre-rib/vertebral and caudal intervertebral disc primordium, respectively (Figure 2D). In Supt20^{hypo} mutants this metameric pattern was disrupted (Figure 2C, D; n=4). Darkly stained cells of the rostral pre-rib/vertebral primordium appeared narrower and in some instances were diffuse and difficult to discern.

The expression pattern of rostral and caudal markers of the somite were visualized by whole mount in situ hybridization. The lower thoracic vertebrae, where fusions are found in Supt20 hypomorphs (T10-13), arise from somites 21-25 that form between E9 and 10 (Gossler and Tam, 2002). Thus, we focused our analyses at E9.5 and 10.5, during and slightly after these

somites are formed. Tbx18 is a T-box transcription factor expressed in the rostral somite (Bussen et al., 2004) and Uncx4.1 is a paired homeobox transcription factor expressed in the caudal somite (Mansouri et al., 1997). Dll1 is a homolog of the Notch ligand Delta and expressed in the caudal half of the somite (Bettenhausen et al., 1995). In control E9.5 and 10.5 embryos, Tbx18 and Uncx4.1/Dll1 display tight localization to the rostral and caudal somite compartments, respectively (Figure 3A, E, E, G). In Supt20 hypomorphs, the Tbx18 expression domain was reduced to varying degrees along the entire anterior-posterior axis in all hypomorphic embryos examined at both E9.5 and 10.5 (n=3 at each stage; Figure 3D, F). Importantly, while the expression domain of Tbx18 was narrower at all levels, expression was dramatically reduced in the prospective thoracic region (Bracket in 3B). Conversely, expression of Uncx4.1 and Dll1 was slightly expanded within individual somites (n=3; Figure 3I-N). Thus, Supt20 hypomorphs exhibit a reduction of rostral somite identity accompanied by a slight expansion of the caudal domain.

Cycling of Notch signaling in the PSM of Supt20 hypomorphs. Somite periodicity as well as rostrocaudal polarity is determined by oscillations of Notch signaling within the posterior PSM (Forsberg et al., 1998; Oginuma et al., 2010; Palmeirim et al., 1997; Shifley et al., 2008). Thus, we determined whether cyclic expression of Notch target genes (Lfng and Hes7) occurs in the PSM of Supt20^{hypo} mutants. While fusions in Supt20^{hypo} mutants are primarily seen in the T10-13 segments of the axial skeleton, the underlying disruption of rostrocaudal somite patterning is seen in all segments that arise from E9.0 onwards (Figure 3). Based on this, subsequent analyses were conducted between E9.5-10.5 and similar results were obtained no matter what stage was analyzed. Expression patterns of both Lfng (Figure 4D-F) and Hes7 (Figure 4A-B) were equally distributed between the three phases of the somite cycle in both wild type and Supt20^{hypo} embryos suggesting that cyclic activation of the Notch pathway was not affected. Interestingly, the intensity of Lfng expression was reduced in all phases of the somite cycle in the PSM of the majority (72%; 18/25) of the Supt20^{hypo} mutants examined. In contrast, the intensity of Hes7 expression was unchanged in the PSM. Additionally, at the determination front where rostrocaudal polarity of the forming somites is determined, expression of Lfng was dramatically decreased in the rostral somite and Hes7 expanded in the caudal somite in Supt20 hypomorphs.

Altered rostrocaudal pattern in the anterior PSM of Supt20^{hypo} mutants. Lfng expression in the rostral half of the newly formed somite is required for proper rostrocaudal patterning (Evrard et al., 1998; Zhang and Gridley, 1998) and reduced Lfng expression here in Supt20 hypomorphs (Figure 4A-C) may contribute to altered rostrocaudal somite patterning. While in the posterior PSM expression of Lfng is induced by Notch signaling, at the determination front the bHLH transcription factor Mesp2 controls Lfng expression (Morimoto et al., 2005). Thus expression of Mesp2 was examined to determine if decreased Lfng expression here might be due to reduced Mesp2 expression. However, no difference in pattern or level of Mesp2 expression was found in Supt20 hypomorphs versus wild type littermates. Approximately one third of Supt20 hypomorphs and littermate controls showed high levels of Mesp2 expression in the rostral and caudal S-1 somite (Figure 5A, B), another third exhibited expression restricted to the rostral compartment of S-1 somite (Figure 5C, D) and the final third showed weak expression in rostral S-1 and S0 (Figure 5E, F). There was no

appreciable difference in expression levels of Mesp2 between Supt20 hypomorphs and wild type littermates in any of these phases.

Mesp2 controls expression of a gene regulatory network that divides the presomite into rostral and caudal domains (reviewed in (Saga, 2012). Mesp2 induces expression of Ripply2, which in turn represses Mesp2 expression in the caudal somite (Takahashi et al., 2010). Ripply2 expression appears as a single intense band in the S-1 somite in approximately half of the wild type embryos (Figure 5G) and the remaining embryos display intense expression in S-1 and weaker expression in S0 (Figure 5I). Ripply2 was expressed in S-1 in half of the Supt20 hypomorphs (7/15) examined (Figure 5H). Half of these (4/7) showed weak expression and the remaining mutants (8/15), showed weak Ripply2 expression in S-1, with comparably greater expression in S0 (Figure 5J). Additional markers of the rostral somite were also reduced in the anterior PSM of Supt20 hypomorphs including of Mesp1 (n=10/13; Figure 5K, L) and Dll3 (n=4/4; Figure 5M, N). Conversely, expression of EphrinB2 in the caudal somite was expanded (n=7/7; Figure 5O, P).

Wnt and Fgf signaling appear unaltered in Supt20 hypomorphs. Activation of Notch signaling in the posterior PSM and translation of these signals to somite formation and patterning requires coordinated activation of the Wnt and Fgf pathways (Benazeraf and Pourquie, 2013; Geetha-Loganathan et al., 2008; Pourquie, 2011). To determine if these are altered in Supt20 hypomorphs, expression of a sampling of ligands and downstream targets were examined. No difference was found in expression of beta-galactosidase in the PSM of BAT-Gal Wnt-reporter embryos (n=2; Figure 6A,B); in expression of the Wnt target gene Brachyury (n=3; Figure 6C, D) nor the Wnt ligand Wnt3a (n=3; Figure 6E, F). Similarly, Fgf8 (n=3; Figure 6G, H) and expression of the Fgf-induce Spry4 transcript (n=16; Figure 6 I, J) appeared unchanged in the PSM of Supt20 hypomorphs. These results suggest that reduction of Lfng expression and the subsequent altered specification of rostrocaudal somite polarity in Supt20 hypomorphs is not likely due to alteration of Wnt or Fgf signaling.

Commonalities in phenotypes between Spt20 and Gcn5 hypomorphs. Supt20 is an essential core component of the Gcn5 containing SAGA complex (Grant et al., 1997; Nagy et al., 2009; Wang et al., 2008). Like hypomorphic Supt20 mutants, Gcn5 hypomorphs show neural tube closure defects along with rib fusions and homeotic transformations (including L1-T14) in the lower thoracic region reminiscent of those described here in Supt20 hypomorphs (Bu et al., 2007; Lin et al., 2008a; Lin et al., 2008b; Zohn et al., 2006). Axial skeletal defects in the lower thoracic region of Gcn5 hypomorphs were attributed to alterations in Hox gene expression but rostrocaudal somite patterning was not examined (Lin et al., 2008a). Specifically, posterior shifts in Hoxc8 and Hoxc9 expression preceded axial skeletal defects in Gcn5 hypomorphs (Lin et al., 2008a). As many Supt20 hypomorphs also show homeotic transformation of L1 to T14, we determined if the shifts in Hoxc8 and Hoxc9 expression observed in Gcn5 hypomorphs (Lin et al., 2008a) also occur in Supt20 mutants. In wild type embryos, Hoxc8 expression is detected in segments posterior to prevertebra V17 that contributes to thoracic vertebrae T5 and T6 (Figure 7A), whereas expression of Hoxc8 in Supt20 hypomorphic mutants was shifted by one segment and detected in segments posterior to and including prevertebra V18 that contributes to thoracic vertebrae T6 and T7 (Figure 7B). Similarly, Hoxc9 was expressed in segments posterior to

and including prevertebra V19 that contribute to thoracic vertebrae T7 and T8 in wild type embryos; whereas expression of Hoxc9 was shifted posteriorly by one segment to prevertebra V20 that contribute to thoracic vertebrae T8 and T9 (Figure 7C, D).

Hox gene expression is initiated during gastrulation in the primitive streak and final expression domains become fixed as cells move through the PSM (Cordes et al., 2004; Dubrulle et al., 2001; Greco et al., 1996; Ikeya and Takada, 2001; Kessel and Gruss, 1991; Lohnes et al., 1994; Partanen et al., 1998; Zakany et al., 2001). Supt20 null mutant embryos show defects in gastrulation resulting in delayed mesoderm migration (Zohn et al., 2006). To determine if posterior shifts in Hoxc8 expression originate when gene expression is initiated during gastrulation, in situ hybridization was done to examine Hoxc8 expression in early somite stage embryos (2-6 somites, n=9). As shown in Figure 7E-H, the expression domain of Hoxc8 appears similar in Supt20 hypomorphic mutant embryos and wild type littermates. Unexpectedly, the intensity of expression was increased in some hypomorphs (5/9). This result indicates that the initiation of Hoxc8 expression is not delayed or shifted anteriorly in E8.5 Supt20 hypomorphs and that the posterior shifts in Hoxc8 expression in E10.5 embryos is more likely due to alteration of signals in the PSM.

To determine if Gcn5 hypomorphic mutants show similar defects in rostrocaudal somite patterning as Supt20 hypomorphs, expression of Tbx18 was examined in $Gcn5^{flox(neo)/flox(neo)}$ mutants. As shown in Figure 7E and F, both the intensity and domain of Tbx18 expression in the rostral somite is reduced in Gcn5 hypomorphs. Similar to Supt20 hypomorphs, reduced expression of Tbx18 was greater in somites that contribute to the thoracic vertebrae (Figure 7F). Thus Gcn5 and Supt20 hypomorphs show similar alterations in rostrocaudal somite patterning and Hoxc gene expression.

Discussion

Supt20 hypomorphic mutants show rib and vertebrae fusions along with L1 to T14 transformations. These defects are preceded by reduced Lfng expression in the posterior PSM, alterations of rostrocaudal somite pattern at the determination front and a posterior shift of Hoxc8 and Hoxc9 expression. Rostrocaudal patterning of the somites requires cyclic activation of Notch, Wnt and Fgf pathways in the posterior PSM (Pourquie, 2011; Saga, 2012). While cycling of Notch target genes and activation of Wnt and Fgf pathways in the posterior PSM appears normal in Supt20 hypomorphs, Lfng expression is reduced in both the posterior and anterior PSM. Mesp2 controls Lfng expression in the anterior PSM and initiates expression of gene networks that specify the rostral presomite including Lfng, Ripply2, Mesp1 and Dll3 (Saga, 2012). Expressions of all of these transcripts are reduced in Supt20 hypomorphs. Together these results suggest that Supt20 is required for full activation of Lfng expression in the posterior PSM and downstream of Mesp2 in the anterior PSM for proper establishment of rostrocaudal somite patterning.

Axial skeletal defects are in Supt20 hypomorphs are primarily localized to the lower thoracic region. Interestingly, fusions of skeletal elements are only observed in the lower thoracic region in Supt20 hypomorphs. Since Supt20 is ubiquitously expressed along the anterior posterior axis of the mouse embryo during somitogenesis (Zohn 2006), the bias in

axial level of skeletal fusions is not likely due to restricted expression but rather, a consequence of the specific pathways regulated by Supt20. While only a few studies are published, Supt20 has multiple context dependent functions. Supt20 was originally found in a yeast two-hybrid screen to identify proteins that bind p38 MAPK (Zohn et al., 2006). Furthermore, p38 MAPK activation in the primitive streak is required for downregulation of E-Cadherin protein allowing for timely migration of mesoderm (Zohn et al., 2006). Subsequently, Supt20 was implicated in regulation of Atg9 during autophagy (Wang et al., 2008; Webber and Tooze, 2010). Of particular interest, both Supt20 and it yeast homologue, Spt20 are essential core components of the Gcn5-containing SAGA complex (Grant et al., 1997; Nagy et al., 2009; Wang et al., 2008). siRNA mediated knockdown of Supt20 results in destabilization of the Gcn5-containing SAGA complex and degradation of Gcn5 (Liu et al., 2013). Since Gcn5 and Supt20 hypomorphs show similar neural tube (exencephaly and spina bifida) and axial skeleton defects (rib fusions and homeotic transformations of lower thoracic segments) (Lin et al., 2008a; Lin et al., 2008b), we explored whether these gross phenotypic similarities are preceded by similar molecular alterations in gene expression. We demonstrate that like Supt20, Gcn5 hypomorphs show reduction of the Tbx18 positive rostral somite. Moreover, like Gcn5, Supt20 hypomorphs exhibit posterior shifts in Hoxc8 and Hoxc9 expression, two Hox genes important for specifying the identity of thoracic segments of the axial skeleton (Le Mouellic et al., 1992; Suemori et al., 1995; van den Akker et al., 2001). Thus it is possible that the axially localized disruption of skeletal development in Supt20 and Gcn5 hypomorphs represents the intersection of altered rostrocaudal somite patterning and expression of Hox genes that specify the lower thoracic segments.

Axial skeletal defects and alteration of Hox gene expression. We previously showed that Supt20 is ubiquitously expressed during gastrulation and somitogenesis (Zohn et al., 2006). Furthermore, Supt20 null mutants show gastrulation defects where mesoderm is properly specified yet migration is delayed due to failure to efficiently down regulate the E-Cadherin protein (Zohn et al., 2006). Patterning of the axial skeleton is initiated at this early time point with induction of temporally collinear Hox gene expression before the nascent mesoderm migrates through the primitive streak (Forlani et al., 2003; Gaunt and Strachan, 1996; Iimura and Pourquie, 2006). Thus delayed mesoderm migration in Supt20 mutant embryos could potentially influence initiation of Hox gene expression accounting for the posterior shift in Hoxc8 and Hoxc9 and anterior transformations. This was initially proposed as a potential mechanism underlying anterior transformations and posterior shifts in Hox expression in Fgfr1 hypomorphs (Partanen et al., 1998). Like Supt20, Fgfr1 is required in the primitive streak for timely mesoderm migration (Ciruna et al., 1997; Zohn et al., 2006). However, analysis of mutants where the Fgfr1 ligands Fgf4 and Fgf8 are conditionally deleted after mesoderm migration results in similar posterior transformations (Naiche et al., 2011), suggesting that disruption of Fgf signals in the PSM rather than at the primitive streak are the likely culprits mediating homeotic transformations. We demonstrate that initiation of Hoxc8 expression is not delayed in Supt20 hypomorphs and that Hoxc8 is expressed at higher levels in many mutant embryos. This result is inconsistent with the posterior shift in expression observed at later stages. However, the final pattern of Hox gene expression is not solely due to initiation of expression at gastrulation, but becomes modified in the PSM

before somite formation (Cordes et al., 2004; Zakany et al., 2001). Furthermore, very few Supt20 hypomorphs showed gastrulation phenotypes whereas somite/vertebrae phenotypes were fully penetrant. Thus, a more likely explanation is that Supt20 is required in the PSM for refinement of Hox gene expression and subsequent axial skeletal patterning. While Wnt and Fgf signaling appear unaffected in Supt20 mutants, Lfng in the posterior PSM was reduced. Intriguingly, reduced Notch signaling in the PSM results in anterior shifts in Hox gene expression and posterior homeotic transformations (Cordes et al., 2004).

Finally, molecular interactions and phenotypic similarities between Gcn5 and Supt20 hypomorphic mutants suggest a common pathway. Like Supt20, Gcn5 is required during gastrulation but for specification rather than migration of mesoderm (Xu et al., 2000; Zohn et al., 2006). Thus, it is unlikely that similarities in phenotype reflect shared functions during gastrulation. Resolution of the precise timing of the requirement for Supt20 action in axial skeletal development awaits creation of conditional alleles and analysis of axial patterning when deleted in the paraxial mesoderm following gastrulation.

Are rostral-caudal pattern defects in Supt20 mutants due to activity at the determination front? Lfng expression is also reduced in Supt20 hypomorphs at the determination front. Here Mesp2 controls Lfng expression, initiating expression of gene networks including Lfng, Ripply2, Mesp1 and Dll3 to specify the rostral somite (reviewed in (Saga, 2012). The initial activation of Mesp2 at the determination front is controlled by the somite clock (Morimoto et al., 2005; Yasuhiko et al., 2006) and was unaffected in Supt20 hypomorphs. In contrast, the downstream gene network specifying rostral versus caudal somite identity was impaired. These results suggest that Supt20 acts at the determination front to establish rostrocaudal somite pattern downstream from Mesp2.

Are axial skeletal defects in Supt20 mutants due to disruption of the Gcn5 containing SAGA complex? The Gcn5 containing SAGA complex may act as a co-activator of Notch induced transcription (Bray, 2006; Fryer et al., 2002; Kitagawa et al., 2001; Kurooka and Honjo, 2000; Petcherski and Kimble, 2000a, b). For example, in Drosophila, the failure to recruit the SAGA complex can enhance the phenotype of Notch pathway mutants (Gause et al., 2006). Interaction with Notch signaling might also explain the effect of Supt20 mutation on rostrocaudal somite pattern at the determination front and Hoxc8 and Hoxc9 gene expression in the PSM. Furthermore, the SAGA complex may interact with Mesp2 to regulate Notch activity. In support of this, Mesp2 inhibits Notch activity in the rostral somite by a mechanism involving destabilization of mastermind-like1 (MamL1), a core component of the nuclear NICD1 complex (Oyama et al., 2011; Sasaki et al., 2011). In Drosophila interactions between MamL function and the SAGA complex in Notch signaling have been documented (Gause et al., 2006; Rollins et al., 1999).

However, subtle differences in phenotype between Supt20 and Gcn5 hypomorphs suggest that this model is likely oversimplified. Rib fusions occur in distal ribs close to the sternum in Gcn5 hypomorphs (Lin et al., 2008a), whereas fusions in Supt20 mutants are found in the proximal ribs adjacent to the vertebrae. Additionally, Supt20 hypomorphs show vertebral fusions while Gcn5 mutants do not (Lin et al., 2008a). Thus it is possible that Gcn5-independent, Supt20-regulated pathways also contribute to axial skeletal defects. Supt20 is

required for p38 MAPK activation in the primitive streak p38 MAPK and intersects with both Transforming Growth Factor beta (Tgfj3) and Wnt signaling pathways important for axial skeletal development (Bikkavilli et al., 2008; Clements et al., 2011; Zohn et al., 2006). For instance, p38 MAPK is activated by the Tgfj3 family ligand Nodal during specification of the anterior visceral endoderm and Supt20 can interact with Nodal to regulate this pathway (Clements et al., 2011). Furthermore, mutation of the Tgfj3 family ligand Gdf11 or its receptors results in homeotic transformations and alterations in Hox gene expression (Andersson et al., 2006; McPherron et al., 1999; Nakashima et al., 1999; Oh and Li, 1997; Oh et al., 2002). On the other hand, experiments in cell lines suggests activation of p38 MAPK can promote and inhibition attenuate canonical Wnt pathway activation (Bikkavilli et al., 2008). Interestingly, hypomorphic Wnt3a mutants show posterior shift of Hox genes along with homeotic transformations of the thoracic and lumbar segments (Greco et al., 1996; Ikeya and Takada, 2001). However, activation of a canonical Wnt reporter in Supt20 hypomorphs was not altered nor was expression of the Wnt3a target gene Brachyury (T) in Supt20 null mutants arguing against disruption of canonical Wnt signaling (Yamaguchi et al., 1999; Zohn et al., 2006). Disruption of non-canonical Wnt pathways could play a role, as double knockout of the non-canonical Wnt5a and Wnt11 genes results in loss of caudal somite fate and similar changes in the Mesp2-initiated gene regulatory network as found in Supt20 mutants (Andre et al., 2015). Additionally, activation of p38 MAPK was reduced in the posterior regions of Wnt5a;Wnt11 double knockout embryos and Wnt5a and Wnt11 can activate p38 MAPK in primary mouse embryonic fibroblasts (Andre et al., 2015).

The origin of axial defects in Supt20 hypomorphic mutants is likely complex. In this study, specific steps in axial skeletal development that require Supt20 gene function are identified. Yet, Supt20 is required early in the mesoderm lineage for proper gastrulation, which might have long lasting implications on subsequent mesoderm and somite development. Additionally, Supt20 regulates multiple pathways that might contribute in different ways to the axial skeletal development. Future experiments will further investigate the relative contribution of these pathways to further elucidate the molecular mechanisms underlying skeletal defects in Supt20 hypomorphs.

Supplementary Material

Refer to Web version on PubMed Central for supplementary material.

Acknowledgements

This work was partially supported by a Basil O'Connor Starter Scholar Research Award from the March of Dimes (5-FY08-23) and a Young Investigator Award from the Spina Bifida Association to I.E.Z. Additional support for this project comes from Award Number 1U54HD090257-01 from the NIH, District of Columbia Intellectual and Developmental Disabilities Research Center Award (DC-IDDRC) program and UL1RR031988 from the National Center for Research Resources. Its contents are solely the responsibility of the authors and do not necessarily represent the official views of the District of Columbia Intellectual and Developmental Disabilities Research Center or the National Institutes of Health. The anti-neurofilament (2H3) antibody was developed by Thomas M. Jessell and Jane Dodd and obtained from the Developmental Studies Hybridoma Bank, created by the NICHD of the NIH and maintained at The University of Iowa, Department of Biology, Iowa City, IA 52242.

References

Andersson O, Reissmann E, Ibanez CF. Growth differentiation factor 11 signals through the transforming growth factor-beta receptor ALK5 to regionalize the anterior-posterior axis. EMBO reports. 2006; 7:831–837. [PubMed: 16845371]

Andre P, Song H, Kim W, Kispert A, Yang Y. Wnt5a and Wnt11 regulate mammalian anterior-posterior axis elongation. Development. 2015; 142:1516–1527. [PubMed: 25813538]

Aoyama H, Asamoto K. The developmental fate of the rostral/caudal half of a somite for vertebra and rib formation: experimental confirmation of the resegmentation theory using chick-quail chimeras. Mech Dev. 2000; 99:71–82. [PubMed: 11091075]

Aulehla A, Johnson RL. Dynamic expression of lunatic fringe suggests a link between notch signaling and an autonomous cellular oscillator driving somite segmentation. Dev Biol. 1999; 207:49–61. [PubMed: 10049564]

Aulehla A, Wehrle C, Brand-Saberi B, Kemler R, Gossler A, Kanzler B, Herrmann BG. Wnt3a plays a major role in the segmentation clock controlling somitogenesis. Dev Cell. 2003; 4:395–406. [PubMed: 12636920]

Aulehla A, Wiegraebe W, Baubet V, Wahl MB, Deng C, Taketo M, Lewandoski M, Pourquie O. A beta-catenin gradient links the clock and wavefront systems in mouse embryo segmentation. Nature cell biology. 2008; 10:186–193. [PubMed: 18157121]

Bagnall KM, Higgins SJ, Sanders EJ. The contribution made by a single somite to the vertebral column: experimental evidence in support of resegmentation using the chick-quail chimaera model. Development. 1988; 103:69–85. [PubMed: 3197634]

Benazeraf B, Pourquie O. Formation and segmentation of the vertebrate body axis. Annual review of cell and developmental biology. 2013; 29:1–26.

Bergemann AD, Cheng HJ, Brambilla R, Klein R, Flanagan JG. ELF-2, a new member of the Eph ligand family, is segmentally expressed in mouse embryos in the region of the hindbrain and newly forming somites. Mol Cell Biol. 1995; 15:4921–4929. [PubMed: 7651410]

Bessho Y, Hirata H, Masamizu Y, Kageyama R. Periodic repression by the bHLH factor Hes7 is an essential mechanism for the somite segmentation clock. Genes Dev. 2003; 17:1451–1456. [PubMed: 12783854]

Bessho Y, Sakata R, Komatsu S, Shiota K, Yamada S, Kageyama R. Dynamic expression and essential functions of Hes7 in somite segmentation. Genes Dev. 2001; 15:2642–2647. [PubMed: 11641270]

Bettenhausen B, Hrabe de Angelis M, Simon D, Guenet JL, Gossler A. Transient and restricted expression during mouse embryogenesis of Dll1, a murine gene closely related to Drosophila Delta. Development. 1995; 121:2407–2418. [PubMed: 7671806]

Bikkavilli RK, Feigin ME, Malbon CC. p38 mitogen-activated protein kinase regulates canonical Wnt-beta-catenin signaling by inactivation of GSK3beta. Journal of cell science. 2008; 121:3598–3607. [PubMed: 18946023]

Biris KK, Dunty WC Jr. Yamaguchi TP. Mouse Ripply2 is downstream of Wnt3a and is dynamically expressed during somitogenesis. Dev Dyn. 2007; 236:3167–3172. [PubMed: 17937396]

Bone RA, Bailey CS, Wiedermann G, Ferjentsik Z, Appleton PL, Murray PJ, Maroto M, Dale JK. Spatiotemporal oscillations of Notch1, Dll1 and NICD are coordinated across the mouse PSM. Development. 2014; 141:4806–4816. [PubMed: 25468943]

Bray SJ. Notch signalling: a simple pathway becomes complex. Nat Rev Mol Cell Biol. 2006; 7:678–689. [PubMed: 16921404]

Bronner-Fraser M. Rostrocaudal differences within the somites confer segmental pattern to trunk neural crest migration. Current topics in developmental biology. 2000; 47:279–296. [PubMed: 10595308]

Bu P, Evrard YA, Lozano G, Dent SY. Loss of Gcn5 acetyltransferase activity leads to neural tube closure defects and exencephaly in mouse embryos. Mol Cell Biol. 2007; 27:3405–3416. [PubMed: 17325035]

Burke AC, Nelson CE, Morgan BA, Tabin C. Hox genes and the evolution of vertebrate axial morphology. Development. 1995; 121:333–346. [PubMed: 7768176]

Bussen M, Petry M, Schuster-Gossler K, Leitges M, Gossler A, Kispert A. The T-box transcription factor Tbx18 maintains the separation of anterior and posterior somite compartments. Genes Dev. 2004; 18:1209–1221. [PubMed: 15155583]

Christ B, Huang R, Scaal M. Formation and differentiation of the avian sclerotome. Anat Embryol (Berl). 2004; 208:333–350. [PubMed: 15309628]

Christ B, Huang R, Scaal M. Amniote somite derivatives. Dev Dyn. 2007; 236:2382–2396. [PubMed: 17557304]

Ciruna B, Rossant J. FGF signaling regulates mesoderm cell fate specification and morphogenetic movement at the primitive streak. Dev Cell. 2001; 1:37–49. [PubMed: 11703922]

Ciruna BG, Schwartz L, Harpal K, Yamaguchi TP, Rossant J. Chimeric analysis of fibroblast growth factor receptor-1 (Fgfr1) function: a role for FGFR1 in morphogenetic movement through the primitive streak. Development. 1997; 124:2829–2841. [PubMed: 9226454]

Clements M, Pernaute B, Vella F, Rodriguez TA. Crosstalk between Nodal/activin and MAPK p38 signaling is essential for anterior-posterior axis specification. Curr Biol. 2011; 21:1289–1295. [PubMed: 21802298]

Cooke J, Zeeman EC. A clock and wavefront model for control of the number of repeated structures during animal morphogenesis. Journal of theoretical biology. 1976; 58:455–476. [PubMed: 940335]

Cordes R, Schuster-Gossler K, Serth K, Gossler A. Specification of vertebral identity is coupled to Notch signalling and the segmentation clock. Development. 2004; 131:1221–1233. [PubMed: 14960495]

Dale JK, Maroto M, Dequeant ML, Malapert P, McGrew M, Pourquie O. Periodic notch inhibition by lunatic fringe underlies the chick segmentation clock. Nature. 2003; 421:275–278. [PubMed: 12529645]

Davis CA, Holmyard DP, Millen KJ, Joyner AL. Examining pattern formation in mouse, chicken and frog embryos with an En-specific antiserum. Development. 1991; 111:287–298. [PubMed: 1680044]

Deng CX, Wynshaw-Boris A, Shen MM, Daugherty C, Ornitz DM, Leder P. Murine FGFR-1 is required for early postimplantation growth and axial organization. Genes Dev. 1994; 8:3045–3057. [PubMed: 8001823]

Dequeant ML, Glynn E, Gaudenz K, Wahl M, Chen J, Mushegian A, Pourquie O. A complex oscillating network of signaling genes underlies the mouse segmentation clock. Science. 2006; 314:1595–1598. [PubMed: 17095659]

Dequeant ML, Pourquie O. Segmental patterning of the vertebrate embryonic axis. Nat Rev Genet. 2008; 9:370–382. [PubMed: 18414404]

Deschamps J, van Nes J. Developmental regulation of the Hox genes during axial morphogenesis in the mouse. Development. 2005; 132:2931–2942. [PubMed: 15944185]

Dubrulle J, McGrew MJ, Pourquie O. FGF signaling controls somite boundary position and regulates segmentation clock control of spatiotemporal Hox gene activation. Cell. 2001; 106:219–232. [PubMed: 11511349]

Dubrulle J, Pourquie O. fgf8 mRNA decay establishes a gradient that couples axial elongation to patterning in the vertebrate embryo. Nature. 2004; 427:419–422. [PubMed: 14749824]

Dunty WC Jr. Biris KK, Chalamalasetty RB, Taketo MM, Lewandoski M, Yamaguchi TP. Wnt3a/beta-catenin signaling controls posterior body development by coordinating mesoderm formation and segmentation. Development. 2008; 135:85–94. [PubMed: 18045842]

Dunwoodie SL, Henrique D, Harrison SM, Beddington RS. Mouse Dll3: a novel divergent Delta gene which may complement the function of other Delta homologues during early pattern formation in the mouse embryo. Development. 1997; 124:3065–3076. [PubMed: 9272948]

Evans DJ. Contribution of somitic cells to the avian ribs. Dev Biol. 2003; 256:114–126. [PubMed: 12654296]

Evrard YA, Lun Y, Aulehla A, Gan L, Johnson RL. lunatic fringe is an essential mediator of somite segmentation and patterning. Nature. 1998; 394:377–381. [PubMed: 9690473]

Ewan KB, Everett AW. Evidence for resegmentation in the formation of the vertebral column using the novel approach of retroviral-mediated gene transfer. Experimental cell research. 1992; 198:315–320. [PubMed: 1729137]

Fleming A, Kishida MG, Kimmel CB, Keynes RJ. Building the backbone: the development and evolution of vertebral patterning. Development. 2015; 142:1733–1744. [PubMed: 25968309]

Forlani S, Lawson KA, Deschamps J. Acquisition of Hox codes during gastrulation and axial elongation in the mouse embryo. Development. 2003; 130:3807–3819. [PubMed: 12835396]

Forsberg H, Crozet F, Brown NA. Waves of mouse Lunatic fringe expression, in four-hour cycles at two-hour intervals, precede somite boundary formation. Curr Biol. 1998; 8:1027–1030. [PubMed: 9740806]

Fryer CJ, Lamar E, Turbachova I, Kintner C, Jones KA. Mastermind mediates chromatin-specific transcription and turnover of the Notch enhancer complex. Genes Dev. 2002; 16:1397–1411. [PubMed: 12050117]

Gaunt SJ, Strachan L. Temporal colinearity in expression of anterior Hox genes in developing chick embryos. Dev Dyn. 1996; 207:270–280. [PubMed: 8922526]

Gause M, Eissenberg JC, Macrae AF, Dorsett M, Misulovin Z, Dorsett D. Nipped-A, the Tra1/TRRAP subunit of the Drosophila SAGA and Tip60 complexes, has multiple roles in Notch signaling during wing development. Mol Cell Biol. 2006; 26:2347–2359. [PubMed: 16508010]

Geetha-Loganathan P, Nimmagadda S, Scaal M, Huang R, Christ B. Wnt signaling in somite development. Ann Anat. 2008; 190:208–222. [PubMed: 18417332]

Goldbeter A, Gonze D, Pourquie O. Sharp developmental thresholds defined through bistability by antagonistic gradients of retinoic acid and FGF signaling. Dev Dyn. 2007; 236:1495–1508. [PubMed: 17497689]

Goldstein RS, Kalcheim C. Determination of epithelial half-somites in skeletal morphogenesis. Development. 1992; 116:441–445. [PubMed: 1286618]

Gossler, A.; Tam, PP. Somitogenesis: Segmentation of the paraxial mesoderm and the delineation of tissue compartments. In: Rossant, J.; Tam, PP., editors. Mouse development. Academic Press; San Diego, CA: 2002. p. 127-149.

Grant PA, Duggan L, Cote J, Roberts SM, Brownell JE, Candau R, Ohba R, Owen-Hughes T, Allis CD, Winston F, Berger SL, Workman JL. Yeast Gcn5 functions in two multisubunit complexes to acetylate nucleosomal histones: characterization of an Ada complex and the SAGA (Spt/Ada) complex. Genes Dev. 1997; 11:1640–1650. [PubMed: 9224714]

Greco TL, Takada S, Newhouse MM, McMahon JA, McMahon AP, Camper SA. Analysis of the vestigial tail mutation demonstrates that Wnt-3a gene dosage regulates mouse axial development. Genes Dev. 1996; 10:313–324. [PubMed: 8595882]

Hogan, B.; Beddington, RS.; Costantini, F.; Lacy, E. Manipulating the Mouse Embryo, a Laboratory Manual. Cold Spring Harbor Laboratory Press; 1994.

Hubaud A, Pourquie O. Signalling dynamics in vertebrate segmentation. Nat Rev Mol Cell Biol. 2014; 15:709–721. [PubMed: 25335437]

Iimura T, Denans N, Pourquie O. Establishment of Hox vertebral identities in the embryonic spine precursors. Current topics in developmental biology. 2009; 88:201–234. [PubMed: 19651306]

Iimura T, Pourquie O. Collinear activation of Hoxb genes during gastrulation is linked to mesoderm cell ingression. Nature. 2006; 442:568–571. [PubMed: 16760928]

Ikeya M, Takada S. Wnt-3a is required for somite specification along the anteroposterior axis of the mouse embryo and for regulation of cdx-1 expression. Mech Dev. 2001; 103:27–33. [PubMed: 11335109]

Ishikawa A, Kitajima S, Takahashi Y, Kokubo H, Kanno J, Inoue T, Saga Y. Mouse Nkd1, a Wnt antagonist, exhibits oscillatory gene expression in the PSM under the control of Notch signaling. Mech Dev. 2004; 121:1443–1453. [PubMed: 15511637]

Kessel M, Gruss P. Homeotic transformations of murine vertebrae and concomitant alteration of Hox codes induced by retinoic acid. Cell. 1991; 67:89–104. [PubMed: 1680565]

Keynes RJ, Stern CD. Segmentation in the vertebrate nervous system. Nature. 1984; 310:786–789. [PubMed: 6472458]

Kitagawa M, Oyama T, Kawashima T, Yedvobnick B, Kumar A, Matsuno K, Harigaya K. A human protein with sequence similarity to Drosophila mastermind coordinates the nuclear form of notch and a CSL protein to build a transcriptional activator complex on target promoters. Mol Cell Biol. 2001; 21:4337–4346. [PubMed: 11390662]

Kraus F, Haenig B, Kispert A. Cloning and expression analysis of the mouse T-box gene Tbx18. Mech Dev. 2001; 100:83–86. [PubMed: 11118889]

Krumlauf R. Hox genes in vertebrate development. Cell. 1994; 78:191–201. [PubMed: 7913880]

Kuan CY, Tannahill D, Cook GM, Keynes RJ. Somite polarity and segmental patterning of the peripheral nervous system. Mech Dev. 2004; 121:1055–1068. [PubMed: 15296971]

Kurooka H, Honjo T. Functional interaction between the mouse notch1 intracellular region and histone acetyltransferases PCAF and GCN5. J Biol Chem. 2000; 275:17211–17220. [PubMed: 10747963]

Le Mouellic H, Lallemand Y, Brulet P. Homeosis in the mouse induced by a null mutation in the Hox-3.1 gene. Cell. 1992; 69:251–264. [PubMed: 1348969]

Lin W, Zhang Z, Chen CH, Behringer RR, Dent SY. Proper Gcn5 histone acetyltransferase expression is required for normal anteroposterior patterning of the mouse skeleton. Development, growth & differentiation. 2008a; 50:321–330.

Lin W, Zhang Z, Srajer G, Chen YC, Huang M, Phan HM, Dent SY. Proper expression of the Gcn5 histone acetyltransferase is required for neural tube closure in mouse embryos. Dev Dyn. 2008b; 237:928–940. [PubMed: 18330926]

Liu X, Xiao W, Wang XD, Li YF, Han J, Li Y. The p38-interacting protein (p38IP) regulates G2/M progression by promoting alpha-tubulin acetylation via inhibiting ubiquitination-induced degradation of the acetyltransferase GCN5. J Biol Chem. 2013; 288:36648–36661. [PubMed: 24220028]

Lohnes D, Mark M, Mendelsohn C, Dolle P, Dierich A, Gorry P, Gansmuller A, Chambon P. Function of the retinoic acid receptors (RARs) during development (I). Craniofacial and skeletal abnormalities in RAR double mutants. Development. 1994; 120:2723–2748. [PubMed: 7607067]

Mansouri A, Yokota Y, Wehr R, Copeland NG, Jenkins NA, Gruss P. Paired-related murine homeobox gene expressed in the developing sclerotome, kidney, and nervous system. Dev Dyn. 1997; 210:53–65. [PubMed: 9286595]

Maretto S, Cordenonsi M, Dupont S, Braghetta P, Broccoli V, Hassan AB, Volpin D, Bressan GM, Piccolo S. Mapping Wnt/beta-catenin signaling during mouse development and in colorectal tumors. Proc Natl Acad Sci U S A. 2003; 100:3299–3304. [PubMed: 12626757]

McGrew MJ, Dale JK, Fraboulet S, Pourquie O. The lunatic fringe gene is a target of the molecular clock linked to somite segmentation in avian embryos. Curr Biol. 1998; 8:979–982. [PubMed: 9742402]

McPherron AC, Lawler AM, Lee SJ. Regulation of anterior/posterior patterning of the axial skeleton by growth/differentiation factor 11. Nat Genet. 1999; 22:260–264. [PubMed: 10391213]

Morimoto M, Takahashi Y, Endo M, Saga Y. The Mesp2 transcription factor establishes segmental borders by suppressing Notch activity. Nature. 2005; 435:354–359. [PubMed: 15902259]

Nagy Z, Riss A, Romier C, le Guezennec X, Dongre AR, Orpinell M, Han J, Stunnenberg H, Tora L. The human SPT20-containing SAGA complex plays a direct role in the regulation of endoplasmic reticulum stress-induced genes. Mol Cell Biol. 2009; 29:1649–1660. [PubMed: 19114550]

Naiche LA, Holder N, Lewandoski M. FGF4 and FGF8 comprise the wavefront activity that controls somitogenesis. Proc Natl Acad Sci U S A. 2011; 108:4018–4023. [PubMed: 21368122]

Nakashima M, Toyono T, Akamine A, Joyner A. Expression of growth/differentiation factor 11, a new member of the BMP/TGFbeta superfamily during mouse embryogenesis. Mech Dev. 1999; 80:185–189. [PubMed: 10072786]

Niederreither K, McCaffery P, Drager UC, Chambon P, Dolle P. Restricted expression and retinoic acid-induced downregulation of the retinaldehyde dehydrogenase type 2 (RALDH-2) gene during mouse development. Mech Dev. 1997; 62:67–78. [PubMed: 9106168]

Niwa Y, Masamizu Y, Liu T, Nakayama R, Deng CX, Kageyama R. The initiation and propagation of Hes7 oscillation are cooperatively regulated by Fgf and notch signaling in the somite segmentation clock. Dev Cell. 2007; 13:298–304. [PubMed: 17681139]

Nomura-Kitabayashi A, Takahashi Y, Kitajima S, Inoue T, Takeda H, Saga Y. Hypomorphic Mesp allele distinguishes establishment of rostrocaudal polarity and segment border formation in somitogenesis. Development. 2002; 29:2473–2481.

Oginuma M, Takahashi Y, Kitajima S, Kiso M, Kanno J, Kimura A, Saga Y. The oscillation of Notch activation, but not its boundary, is required for somite border formation and rostral-caudal patterning within a somite. Development. 2010; 137:1515–1522. [PubMed: 20335362]

Oh SP, Li E. The signaling pathway mediated by the type IIB activin receptor controls axial patterning and lateral asymmetry in the mouse. Genes Dev. 1997; 11:1812–1826. [PubMed: 9242489]

Oh SP, Yeo CY, Lee Y, Schrewe H, Whitman M, Li E. Activin type IIA and IIB receptors mediate Gdf11 signaling in axial vertebral patterning. Genes Dev. 2002; 16:2749–2754. [PubMed: 12414726]

Oyama T, Harigaya K, Sasaki N, Okamura Y, Kokubo H, Saga Y, Hozumi K, Suganami A, Tamura Y, Nagase T, Koga H, Nishimura M, Sakamoto R, Sato M, Yoshida N, Kitagawa M. Mastermind-like 1 (MamL1) and mastermind-like 3 (MamL3) are essential for Notch signaling in vivo. Development. 2011; 138:5235–5246. [PubMed: 22069191]

Palmeirim I, Henrique D, Ish-Horowicz D, Pourquie O. Avian hairy gene expression identifies a molecular clock linked to vertebrate segmentation and somitogenesis. Cell. 1997; 91:639–648. [PubMed: 9393857]

Partanen J, Schwartz L, Rossant J. Opposite phenotypes of hypomorphic and Y766 phosphorylation site mutations reveal a function for Fgfr1 in anteroposterior patterning of mouse embryos. Genes Dev. 1998; 12:2332–2344. [PubMed: 9694798]

Petcherski AG, Kimble J. LAG-3 is a putative transcriptional activator in the C. elegans Notch pathway. Nature. 2000a; 405:364–368. [PubMed: 10830967]

Petcherski AG, Kimble J. Mastermind is a putative activator for Notch. Curr Biol. 2000b; 10:R471–473. [PubMed: 10898989]

Pourquie O. Vertebrate segmentation: from cyclic gene networks to scoliosis. Cell. 2011; 145:650–663. [PubMed: 21620133]

Rashbass P, Cooke LA, Herrmann BG, Beddington RS. A cell autonomous function of Brachyury in T/T embryonic stem cell chimaeras. Nature. 1991; 353:348–351. [PubMed: 1922339]

Roelink H, Nusse R. Expression of two members of the Wnt family during mouse development--restricted temporal and spatial patterns in the developing neural tube. Genes Dev. 1991; 5:381–388. [PubMed: 2001840]

Rollins RA, Morcillo P, Dorsett D. Nipped-B, a Drosophila homologue of chromosomal adherins, participates in activation by remote enhancers in the cut and Ultrabithorax genes. Genetics. 1999; 152:577–593. [PubMed: 10353901]

Saga Y. Segmental border is defined by the key transcription factor Mesp2, by means of the suppression of Notch activity. Dev Dyn. 2007; 236:1450–1455. [PubMed: 17394251]

Saga Y. The mechanism of somite formation in mice. Curr Opin Genet Dev. 2012; 22:331–338. [PubMed: 22742849]

Saga Y, Hata N, Kobayashi S, Magnuson T, Seldin MF, Taketo MM. MesP1: a novel basic helix-loop-helix protein expressed in the nascent mesodermal cells during mouse gastrulation. Development. 1996; 122:2769–2778. [PubMed: 8787751]

Saga Y, Hata N, Koseki H, Taketo MM. Mesp2: a novel mouse gene expressed in the presegmented mesoderm and essential for segmentation initiation. Genes Dev. 1997; 11:1827–1839. [PubMed: 9242490]

Sakai Y, Meno C, Fujii H, Nishino J, Shiratori H, Saijoh Y, Rossant J, Hamada H. The retinoic acid-inactivating enzyme CYP26 is essential for establishing an uneven distribution of retinoic acid along the anterio-posterior axis within the mouse embryo. Genes Dev. 2001; 15:213–225. [PubMed: 11157777]

Sasaki N, Kiso M, Kitagawa M, Saga Y. The repression of Notch signaling occurs via the destabilization of mastermind-like 1 by Mesp2 and is essential for somitogenesis. Development. 2011; 138:55–64. [PubMed: 21098559]

Scaal M. Early development of the vertebral column. Seminars in cell & developmental biology. 2016; 49:83–91. [PubMed: 26564689]

Schuster-Gossler K, Harris B, Johnson KR, Serth J, Gossler A. Notch signalling in the paraxial mesoderm is most sensitive to reduced Pofut1 levels during early mouse development. BMC developmental biology. 2009; 9

Shifley ET, Vanhorn KM, Perez-Balaguer A, Franklin JD, Weinstein M, Cole SE. Oscillatory lunatic fringe activity is crucial for segmentation of the anterior but not posterior skeleton. Development. 2008; 135:899–908. [PubMed: 18234727]

Song J, Oh SP, Schrewe H, Nomura M, Lei H, Okano M, Gridley T, Li E. The type II activin receptors are essential for egg cylinder growth, gastrulation, and rostral head development in mice. Dev Biol. 1999; 213:157–169. [PubMed: 10452853]

Suemori H, Takahashi N, Noguchi S. Hoxc-9 mutant mice show anterior transformation of the vertebrae and malformation of the sternum and ribs. Mech Dev. 1995; 51:265–273. [PubMed: 7547473]

Sun X, Meyers EN, Lewandoski M, Martin GR. Targeted disruption of Fgf8 causes failure of cell migration in the gastrulating mouse embryo. Genes Dev. 1999; 13:1834–1846. [PubMed: 10421635]

Takada S, Stark KL, Shea MJ, Vassileva G, McMahon JA, McMahon AP. Wnt-3a regulates somite and tailbud formation in the mouse embryo. Genes Dev. 1994; 8:174–189. [PubMed: 8299937]

Takahashi J, Ohbayashi A, Oginuma M, Saito D, Mochizuki A, Saga Y, Takada S. Analysis of Ripply1/2-deficient mouse embryos reveals a mechanism underlying the rostro-caudal patterning within a somite. Dev Biol. 2010; 342:134–145. [PubMed: 20346937]

Takahashi Y, Inoue T, Gossler A, Saga Y. Feedback loops comprising Dll1, Dll3 and Mesp2, and differential involvement of Psen1 are essential for rostrocaudal patterning of somites. Development. 2003; 130:4259–4268. [PubMed: 12900443]

Takahashi Y, Koizumi K, Takagi A, Kitajima S, Inoue T, Koseki H, Saga Y. Mesp2 initiates somite segmentation through the Notch signalling pathway. Nat Genet. 2000; 25:390–396. [PubMed: 10932180]

Tanaka A, Miyamoto K, Minamino N, Takeda M, Sato B, Matsuo H, Matsumoto K. Cloning and characterization of an androgen-induced growth factor essential for the androgen-dependent growth of mouse mammary carcinoma cells. Proc Natl Acad Sci U S A. 1992; 89:8928–8932. [PubMed: 1409588]

van den Akker E, Fromental-Ramain C, de Graaff W, Le Mouellic H, Brulet P, Chambon P, Deschamps J. Axial skeletal patterning in mice lacking all paralogous group 8 Hox genes. Development. 2001; 128:1911–1921. [PubMed: 11311170]

Wahl MB, Deng C, Lewandoski M, Pourquie O. FGF signaling acts upstream of the NOTCH and WNT signaling pathways to control segmentation clock oscillations in mouse somitogenesis. Development. 2007; 134:4033–4041. [PubMed: 17965051]

Wang L, Dent SY. Functions of SAGA in development and disease. Epigenomics. 2014; 6:329–339. [PubMed: 25111486]

Wang YL, Faiola F, Xu M, Pan S, Martinez E. Human ATAC Is a GCN5/PCAF-containing acetylase complex with a novel NC2-like histone fold module that interacts with the TATA-binding protein. J Biol Chem. 2008; 283:33808–33815. [PubMed: 18838386]

Webber JL, Tooze SA. Coordinated regulation of autophagy by p38alpha MAPK through mAtg9 and p38IP. Embo J. 2010; 29:27–40. [PubMed: 19893488]

Wellik DM. Hox genes and vertebrate axial pattern. Current topics in developmental biology. 2009; 88:257–278. [PubMed: 19651308]

White PH, Farkas DR, McFadden EE, Chapman DL. Defective somite patterning in mouse embryos with reduced levels of Tbx6. Development. 2003; 130:1681–1690. [PubMed: 12620991]

Xu W, Edmondson DG, Evrard YA, Wakamiya M, Behringer RR, Roth SY. Loss of Gcn5l2 leads to increased apoptosis and mesodermal defects during mouse development. Nat Genet. 2000; 26:229–232. [PubMed: 11017084]

Yamaguchi TP, Takada S, Yoshikawa Y, Wu N, McMahon AP. T (Brachyury) is a direct target of Wnt3a during paraxial mesoderm specification. Genes Dev. 1999; 13:3185–3190. [PubMed: 10617567]

Yasuhiko Y, Haraguchi S, Kitajima S, Takahashi Y, Kanno J, Saga Y. Tbx6-mediated Notch signaling controls somite-specific Mesp2 expression. Proc Natl Acad Sci U S A. 2006; 103:3651–3656. [PubMed: 16505380]

Yusuf F, Brand-Saberi B. The eventful somite: patterning, fate determination and cell division in the somite. Anat Embryol (Berl). 2006; 211(Suppl 1):21–30. [PubMed: 17024302]

Zakany J, Kmita M, Alarcon P, de la Pompa JL, Duboule D. Localized and transient transcription of Hox genes suggests a link between patterning and the segmentation clock. Cell. 2001; 106:207–217. [PubMed: 11511348]

Zhang N, Gridley T. Defects in somite formation in lunatic fringe-deficient mice. Nature. 1998; 394:374–377. [PubMed: 9690472]

Zhang S, Lin Y, Itaranta P, Yagi A, Vainio S. Expression of Sprouty genes 1, 2 and 4 during mouse organogenesis. Mech Dev. 2001; 109:367–370. [PubMed: 11731251]

Zohn IE, Li Y, Skolnik EY, Anderson KV, Han J, Niswander L. p38 and a p38-interacting protein are critical for downregulation of E-cadherin during mouse gastrulation. Cell. 2006; 125:957–969. [PubMed: 16751104]

Highlights

- Hypomorphic Supt20 mutants exhibit defects in axial skeletal development including fusions of ribs and vertebrae and anterior homeotic transformations of lower thoracic segments
- Axial skeletal defects are preceded by altered rostrocaudal patterning of the somite and posterior shift of Hoxc8 and Hoxc9 expression.
- Expression of Lfng is reduced in the posterior PSM, but cycling of Lfng and Hes7 and activation of Fgf and Wnt pathways appear unaffected.
- Activation of the gene regulatory cascade downstream of Mesp2 to establish rostrocaudal somite polarity at the determination front is altered.
- Supt20 interacts with Gcn5 and Gcn5 hypomorphs show similar axial skeletal defects of the lower thoracic region preceded by reduction of the rostral somite and posterior shifts in Hoxc8 and Hoxc9 expression.

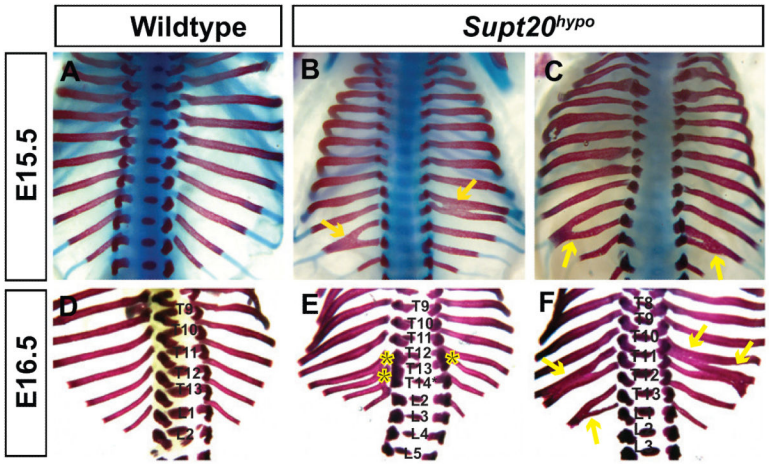

Figure 1.

Supt20 hypomorphs show rib and vertebrae fusions. Dorsal views of Alcian blue/Alizarin red stained skeletons from wild type (A,D) and Supt20^{hypo} embryos (B,C,E,F) at E15.5 (A-C) and E16.5 (D-F). Supt20^{hypo} embryos have rib (yellow arrows) and vertebrae (*) fusions. Thoracic and lumbar vertebrae are labeled (T4-T13 and L1-L5) with L1 to T14 transformations in Supt20^{hypo} embryos labeled as T14* in B, C and E.

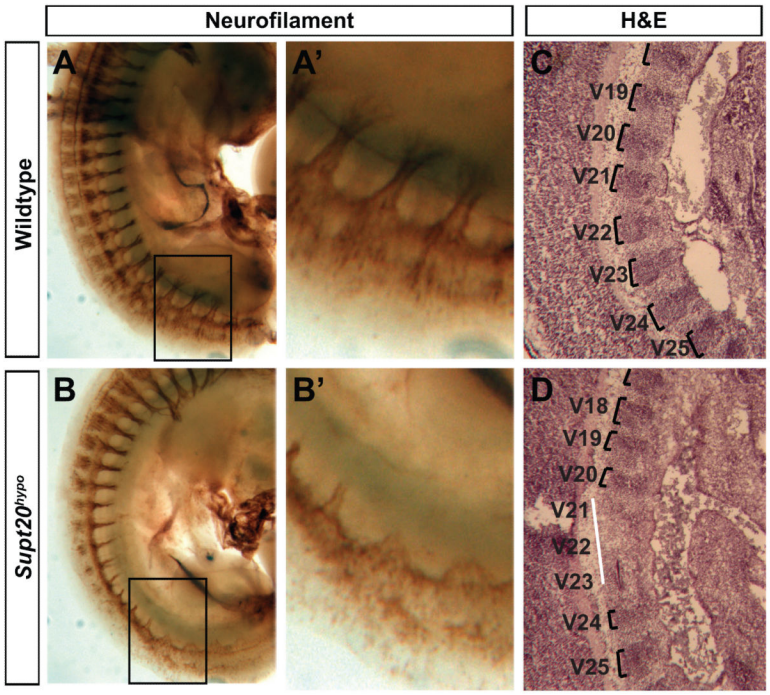

Figure 2.

Disrupted migration of neural crest within somites of Supt20 hypomorphs. A,B. Staining of peripheral nerves with an anti-neurofilament antibody reveals disrupted migration through the rostral somite of E10.5 Supt20 hypomorph (B) but not wild type (A) embryos. Panels A' and B' show magnified views of the boxed regions in A and B. Hematoxylin and Eosin (H&E) staining (C, D) of sagittal sections of E12.5 wild type (C) and Supt20^{hypo} embryos (D) reveals narrowing of the darker stained rostral pre-rib/vertebral (brackets) and expansion of the caudal intervertebral disc primordium. Prevertebra 19-25 that contribute to thoracic vertebrae T7/8 to T13/L1 are labeled V19-V25.

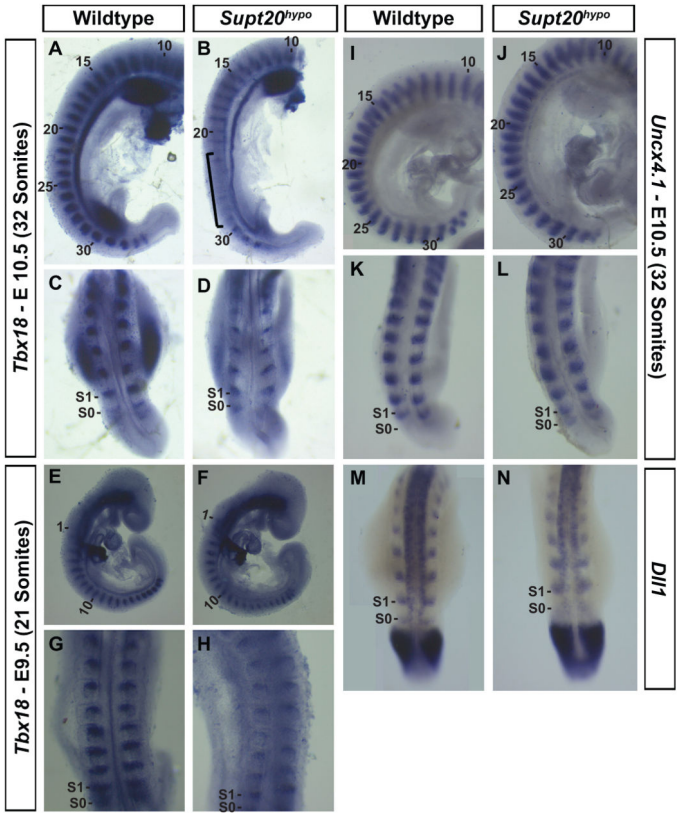

Figure 3.

Altered rostrocaudal patterning of the somites in Supt20 hypomorphs. Expression of Tbx18 (A-H), a marker if the rostral somite, is reduced in E10.5 (A-D) and E9.5 (E-H) Supt20^{hypo} (B, D, F, H) compared to wild type embryos (A, C, E, G). Conversely expression of markers of the caudal somite, Uncx4.1 (I-L) and Dll1 (M, N), are expanded in E10.5 Supt20^{hypo} (J, L, N) compared to wild type littermates (I, K, M). Numbers in panels A, B, E, F, I and J refer to somite numbers. Bracket in B highlights somites that will develop into lower thoracic vertebrae with significantly reduced Tbx18 expression.

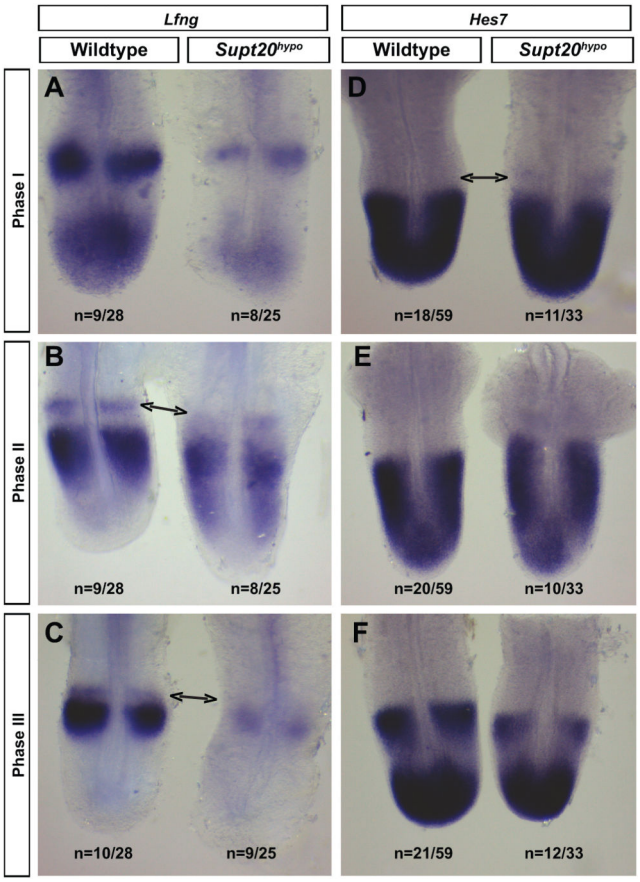

Figure 4.

The somite clock cycles in the PSM of Supt20 hypomorphs, but levels of the Notch target gene Lfng expression are reduced. Approximately equal proportions of E10.5 wild type and Supt20^{hypo} embryos showed Phase I (A, D), Phase II (B, E) and Phase III (C, F) patterns of expression of Lfng (A-C) and Hes7 (D-F). The numbers of embryos with each pattern of expression are indicated. However, the intensity of Lfng, but not Hes7 expression was consistently reduced in the PSM of Supt20^{hypo} embryos. In contrast, Lfng expression was decreased and Hes7 increased at the determination front in Supt20 hypomorphs (arrows in B, C and D).

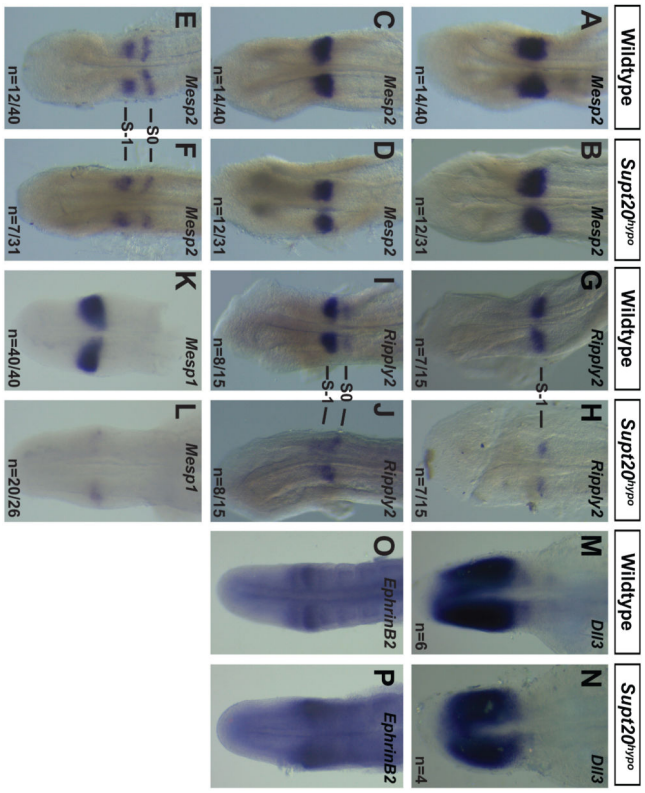

Figure 5.

Altered expression of markers of rostrocaudal somite polarity at the determination front. A-F) Approximately equal numbers of wild type and Supt20^{hypo} embryos showed Phase I (A, B), Phase II (C, D) and Phase III (E, F) patterns of expression of Mesp2 in E9.5 Supt20^{hypo} mutants (B, D, F) compared to littermate controls (A, C, E). The numbers of embryos with each pattern of expression are indicated. Expression levels of Mesp2 were not appreciably different between wild type and hypomorphic mutants (G-J). Ripply2 expression was equally distributed between two phases of expression in E9.5 wild type (G, I) and Supt20 hypomorphs (H, J). However, expression of Ripply2 was reduced in mutants in S-1 in all phases (H and J) but increased in S0 in the second phase (J). Expression of rostral somite markers Mesp1 (E9.5; K, L) and Dll3 (E10.5; M, N) are reduced while the caudal marker EphrinB2 (E10.5; O, P) is expanded in Supt20^{hypo} mutants (L, N, P) compared to wild types (K, M, O). Q). Model showing signaling at the determination front regulating rostrocaudal polarity and where Supt20 fits in based on our data.

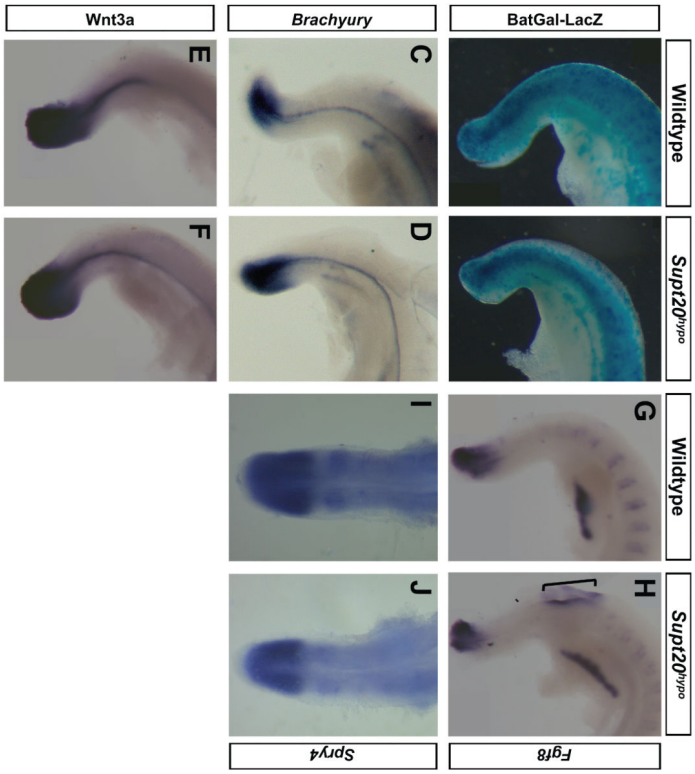

Figure 6.

Wnt and Fgf pathways are not altered in the PSM of Supt20^{hypo} mutants. Activation of the LacZ reporter in embryos expressing the BAT-GAL transgene (A, B) and expression of Brachyury (C, D), Wnt3a (E, F), Fgf8 (G, H) and Spry4 (I, J) are not altered in the PSM of E10.5 Supt20^{hypo} mutants (B, D, F, H, J) compared to wild types (A, C, E, G, I). Embryo in H shows spina bifida (bracket). Note expression of Fgf8 and Spry4 in the rostral somite is reduced in Supt20 hypomorphs (panels H and J).

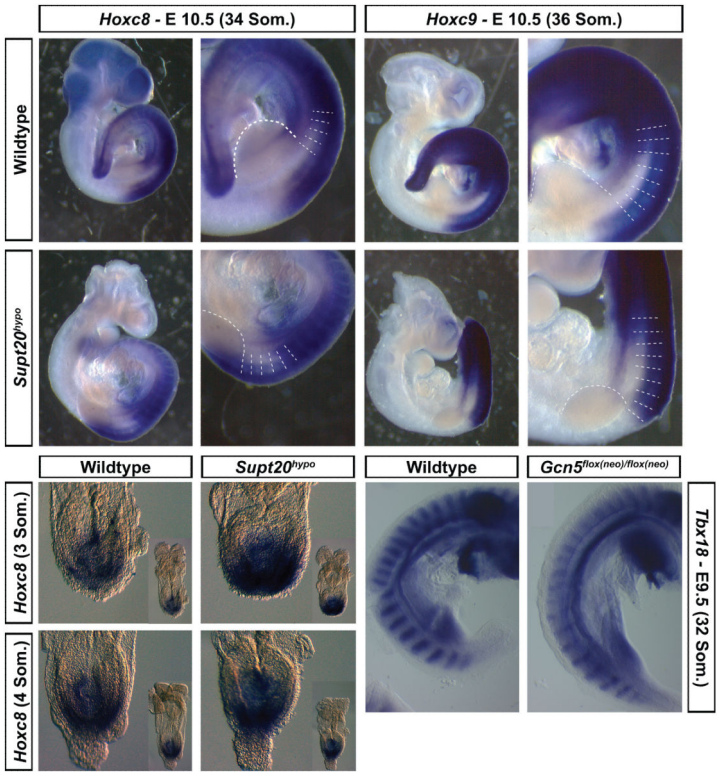

Figure 7.

Commonalities in phenotype between Supt20 and Gcn5 hypomorphs. A-D) Expression of Hoxc8 (A, B) and Hoxc9 (C, D) are shifted in E10.5 Supt20 hypomorphs (B, D; n=2) compared to wild type littermates (A ,C). Panels A'-D' show magnified views of embryos in A-D. Prevertebra 15-21 are labeled as V15 to V21 that contribute to thoracic vertebrae T3/4 to T9/10. (E-H) Expression of Hoxc8 around the primitive streak of E8.5 Supt20 hypomorphs (F, H; n=9) compared to wild type littermates (E, G). Appearance of whole embryo is shown in inset. (I, J) Expression of the rostral somite marker Tbx18 is reduced in E10.5 (E) $Gcn5^{flox(neo)/flox(neo)}$ hypomorphic mutants compared to (F) littermate controls (n=7). Som. = somites